HHS Public Access

Author manuscript

J Phys Chem B. Author manuscript; available in PMC 2016 March 31.

Published in final edited form as:

J Phys Chem B. 2015 July 16; 119(28): 8693–8697. doi:10.1021/acs.jpcb.5b01706.

Conformational changes of the *Hs*DHODH N-terminal Microdomain via DEER Spectroscopy

Eduardo F. Vicente[†], **Indra D. Sahu**[‡], **Antonio J. Costa-Filho**[§], **Eduardo M. Cilli**[‖], and **Gary A. Lorigan**[*,‡]

[†]UNESP – Univ Estadual Paulista, Campus de Tupã, 17602-496, Tupã, SP Brazil

[‡]Department of Chemistry and Biochemistry, Miami University, 45056, Oxford, Ohio United States

[§]Laboratório de Biofísica Molecular, Departamento de Física, Faculdade de Filosofia, Ciências e Letras de Ribeirão Preto, Universidade de São Paulo – USP,14040-901, Ribeirão Preto, SP Brazil

[‖]Departamento de Bioquímica e Tecnologia Química, Instituto de Química, UNESP - Univ Estadual Paulista, 14800-900, Araraquara, SP Brazil

Abstract

The human enzyme dihydroorotate dehydrogenase (*Hs*DHODH) has been studied for being a target for development of new antineoplasic and antiproliferative drugs. The synthetic peptide N-t(DH) represents the N-terminal microdomain of this enzyme, responsible for anchoring it to the inner mitochondrial membrane. Also, it is known to harbor quinones that are essential for enzyme catalysis. Here we report structural features of the peptide/membrane interactions obtained by using CD and DEER spectroscopic techniques, both in micelles and in lipid vesicles. The data revealed different peptide conformational states in micelles and liposomes, which could suggest that this microdomain acts in specific regions or areas of the mitochondria, which can be related with the control of the quinone access to the *Hs*DHODH active site. This is the first study to report on conformational changes of the *Hs*DHODH N-terminal microdomain through a combination of CD and DEER spectroscopic techniques.

Graphical abstract

[*]**Corresponding Author**: (G.A.L.) gary.lorigan@miamioh.edu. Telephone: +1 (513) 529-3338. Fax: +1 (513) 529-5715.

Supporting Information

Initial time domain decay, background correction and L-curves for DEER data in micelle and liposome environments. The Supporting Information is available free of charge on the ACS Publications website at DOI: 10.1021/acs.jpcb.5b01706.

Author Contributions

The manuscript was written through contributions of all authors. All authors have given approval to the final version of the manuscript.

The authors declare no competing financial interest.

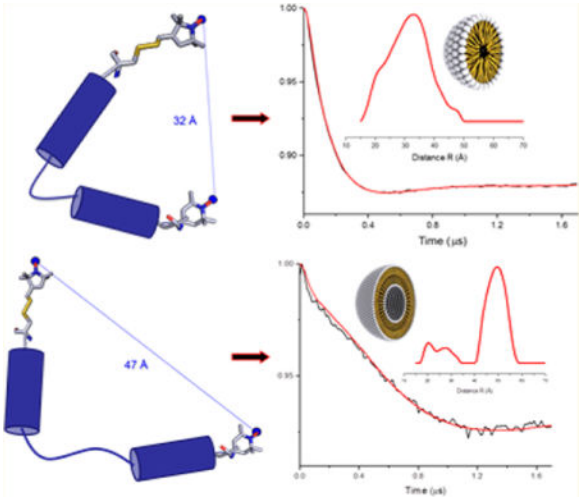

INTRODUCTION

The *Homo sapiens* dihydroorotate dehydrogenase enzyme (*Hs*DHODH - E. C. 1.3.5.2 and PDB ID: 1D3H) acts in the "de novo" pyrimidine biosynthesis pathway catalyzing the oxidation of the (S)-dihydroorotate to orotate in the only redox step of this pathway.[1] The global reaction occurs in two half-reactions: the flavin mononucleotide (FMN) prosthetic group is reduced and, simultaneously, respiratory quinones are oxidized.[2] The latter molecules regenerate the flavin groups, thus working as their physiological electron acceptors.[3] The *Hs*DHODH inhibition decreases pyrimidine production in cells thus inhibiting rapid proliferation,[4] and turned this enzyme into an attractive drug target for the potential treatment of several proliferative diseases, such as cancer and rheumatoid arthritis.[5,6] *Hs*DHODH belongs to DHODH's class 2, which are enzymes associated with membranes through a conserved N-terminal microdomain.[7] Although many studies have highlighted the importance of the *Hs*DHODH active site,[8,9] the N-terminal region also plays a remarkable role in the catalysis: it behaves as an anchor to the membrane, harboring the respiratory quinones for the FMN regeneration and serving as a "main entrance" for the tunnel that leads to the active site.[10] Also, it is essential for the enzyme localization in the inner mitochondrial membrane.[11] However, details on the N-terminal conformation and dynamics upon membrane binding, which could bring new possibilities for the development of drugs for the enzyme inhibition, are still not known.[12,13]

In this work, we studied peptide analogues of the *Hs*DHODH N-terminal microdomain, named N-t(DH), representing the sequence from Gly^{33} to Gly^{66} of the enzyme N-terminus acetyl-GDERFYAEHLMPTLQGLLDPESAHRLAVRFTSLG-$CONH_2$.[14] The *Hs*DHODH protein structure, solved by Liu et al.,[10] showed an N-terminal region containing two alpha-helices (α1 and α2) connected by a loop, forming a hairpin-like structure. Thus, aiming at mimicking that region, we manually synthesized via solid phase peptide synthesis,[15] according to the standard N^{α}-Fmoc protecting group strategy,[16] the N-t(DH) peptide and one analogue containing specific alterations that allowed the molecule to be spin labeled for pulsed electron spin resonance (ESR) studies. This analogue, named [Cys^{35}MTSL-

TOAC^0]N-t(DH), has the MTSL[17] spin label attached to a cysteine added at the C-terminus, while the unnatural spin-labeled amino acid TOAC (2,2,6,6-tetramethylpiperidine-1-oxyl-4-amino-4-carboxylicacid)[18] was added at the N-terminus, labeling both peptide extremes. The N-t(DH) peptide and the analogue were purified and characterized following the standard method described in the Experimental Section.[19] The studies were performed in *n*-dodecylphosphocholine (DPC) micelles and 1-palmitoyl-2-oleoyl-*sn*-glycero-3-phosphocholine (POPC) multilamellar vesicles (MLV) as membrane mimetic environments. Micelles are the simplest membrane mimetic environment, very well established in the literature and used in several studies to evaluate binding and interaction with peptides.[20,21] In the same way, liposomes represent a better membrane model of a lipid bilayer for studying interactions between peptide/protein and membranes.[22–24] In this work, we used circular dichroism (CD) and double electron–electron resonance (DEER) spectroscopic techniques to investigate the structural and conformational features of the peptide and its spin-labeled analogue in the presence of different membrane mimetics.[25–27]

EXPERIMENTAL SECTION

The peptide analogues were manually synthesized by solid phase peptide synthesis following the standard N$^{\alpha}$-Fmoc protecting group strategy. The Rink Amide resin (purchased from Synpep) was employed as the synthesis solid support, containing 0.6 mmol g^{-1} of substitution degree. Deprotection of the *α*-amino group of the resin and amino acids was made with 20% piperidine in dimethylformamide (DMF) in order to remove the base-labile Fmoc protecting group. The amino acid coupling reaction was performed using diisopropylcarbodiimide (DIC)/*N*-hydroxybenzotriazole (HOBt) in methylene chloride (DCM)/DMF approximately 1:1 (v/v) for 2 h stirring and with 3-fold excess for all coupling reagents and amino acids. If necessary, *O*-(benzotriazol-1-yl)-*N*,*N*,*N*′,*N*′-tetramethyluroniumhexafluorophosphate (HBTU)/diisopropylethylamine (DIEA) in DCM/*N*-methylpyrrolidone (NMP) 1:1 (v/v) were used to improve the coupling reaction. The resin was washed with three or four cycle of DCM and DMF for excess reagents and subproducts removal. TOAC incorporation in the analogue [Cys^{35}MTSL-TOAC^0]N-t(DH) was performed with 1.2 mol equiv excess fold, using as acylating reagents 1-[bis(dimethylamino)methylene]-1*H*-1,2,3-triazolo[4,5-*b*]-pyridiniumhexafluorophosphate-3-oxide](HATU)/DIEA with 3.0 and 4.0 mol equiv excess, respectively, in DCM/NMP 1:1 (v:v) solvents over the amino component in the resin. An acetyl group capping was added to the N-terminus and, due to the resin functionalization, the peptides had an amidated C-terminus. The cleavage was performed using trifluoroacetic acid (TFA), triisopropylsilane (TIS) and water (95:2.5:2.5, v:v:v, respectively). The sample was treated with cold diethyl ether and centrifuged three times. The precipitate was resuspended in an aqueous solution, obtaining the crude peptides, which were lyophilizated. The extracted spin-labeled analogue was treated with ammonium hydroxide for complete N–O deprotonation, step monitored by analytical HPLC. After that, peptides purification were performed by semipreparative HPLC Beckman System Gold (Brea, CA) with a reverse phase C-18 column in a linear gradient, flow rate 5 mL/min^{-1}, using aqueous 0.02 mol L^{-1}ammonium acetate (pH 5.0) and 90% acetonitrile in ammonium acetate solution as solvents A and B, respectively.[19] The peptides purity were checked by analytical HPLC Varian (Santa Clara, CA), flow rate of 1.0 mL/

min^{-1}, UV detection at 220 nm, using solvents A (0.045% TFA:H_2O) and B (0.036% TFA:ACN) with a linear gradient of 5–95% (v/v) of solvent B for 30 min. After purification, MTSL attachment was carried out using 5.0 mol equiv excess of the spin label over the analogue [Cys^{35}MTSL-TOAC^0]N-t(DH) in Tris–HCl 0.01 mol L^{-1}, NaCl 0.01 mol L^{-1}, pH 7.4 buffer solution for 4 h stirring. After this procedure, the spin-labeled peptide analogue was purified again following the protocol described above, in order to obtain pure fractions of the molecule. The confirmation of the peptide analogue obtaining was evaluated by Electrospray Mass Spectrometry, on a ZMD Micromass model equipment (Milford, MA).

CD measurements were performed at 25 °C on a Jasco Products Company, Inc. J-715 (Oklahoma City, OK) spectropolarimeter, using a 1 mm path-length quartz cell. Samples containing 30 μmol L^{-1} of peptide analogue were added to a solution containing Tris–HCl 0.01 mol L^{-1}, NaCl 0.01 mol L^{-1}, pH 7.4 buffer solution and 10 mmol L^{-1} of DPC micelles concentration, previously weighted from a powder lipid (Avanti, Alabaster, AL). The liposomes type MLV (Large Multilamellar Vesicles) were prepared using 1-palmitoyl-2-oleoyl-*sn*-glycero-3-phosphocholine (POPC) lipid (Avanti, Alabaster, AL) and added into a flask tube, in a final molar peptide/lipid ratio of 1:250 (maintaining the peptide concentration of 30 μmol L^{-1}) in 300 μL Tris/NaCl buffer solution. The solution was equilibrated by repeating at least 10 freeze–thaw-sonication cycles until the sample became clear. Spectra were acquired every 0.2 nm from 250 to 190 nm at a scan speed of 50 nm min^{-1}, with a 2 nm bandwidth and a response time of 3 s. Each spectrum represents an average of 8 successive scans and is expressed as molar ellipticity [θ] (deg cm^2 dmol^{-1}).

Four pulse DEER experiments were collected using a Bruker ELEXSYS E580 spectrometer equipped with a SuperQ-FT pulse Q-band system with a 10 W amplifier and EN5107D2 resonator, located at the Ohio Advanced EPR Laboratory. All DEER samples were prepared at a spin concentration around 100 μmol L^{-1}. Deuterated glycerol (30% w/w) was used as the sample cryoprotectant. The sample solution was loaded into a 1.1 mm inner diameter quartz capillary (Wilmad-LabGlass, Buena, NJ) and assembled into the sample holder (plastic rod), which was inserted into the resonator cavity. DEER data were collected using the standard four pulse sequence [$(\pi/2)_{\nu 1} - \tau_1 - (\pi)_{\nu 1} - t - (\pi)_{\nu 2} - (\tau_1 + \tau_2 - t) - (\pi)_{\nu 1} - \tau_2$ − echo][28] at Q-band with a probe pulse width of 10/20 ns, pump pulse width of 24 ns, 80 MHz of frequency difference between probe and pump pulse, shot repetition time determined by spin–lattice relaxation time (T_1), 100 echoes/point, and 2-step phase cycling at 80 K collected out to ~2.0 μs for overnight data acquisition time. DEER data were analyzed using DEER Analysis 2013.[29] The distance distributions $P(r)$ were obtained by Tikhonov regularization[30] in the distance domain, incorporating the constraint $P(r) > 0$ under DEER Analysis 2013. A homogeneous three-dimensional model for micelles and a homogeneous two-dimensional model for liposomes were used for background correction. The regularization parameter in the L-curve was optimized by carefully examining the best fit of the time domain.

RESULTS AND DISCUSSION

CD spectroscopy was performed to study the secondary structure of the peptide in a DPC micelle and in a lipid bilayer (liposomes). Previous work on the N-t(DH) peptide in aqueous

solution has indicated a predominantly disordered structure.[14] In DPC micelles (Figure 1), the peptides exhibited a spectrum attributed mainly to an α helix structure (negative peak at 208 and 222 nm and positive peak near 195 nm). Interestingly, when compared to spectra measured in POPC liposomes (Figure 1), it is clear the amount of α helix that peptide N-t(DH) acquired in this environment has changed, increasing the percentage of nonhelical disordered structures. The shifted bands of the peptides in liposomes near 205 nm were already observed in the literature and can be described as partially helical or short α-helical structures.[31,32] In our case, we believe that the band is also a contribution of random structures from a nonbinding portion of peptide N-t(DH) in POPC liposomes. Previous studies with N-t(DH) peptide described a direct transition from a random coil in solution to an α-helical type of structure in SDS and LPC micelles,[14] which can explain the partial structuration of peptide N-t(DH) in POPC liposomes.

To further analyze these structural differences due to the environment on the studied peptide, the molar ellipticities ratios at 222 and 208 nm ($[\theta]_{222}/[\theta]_{208}$)[33] of the peptide CD curves in both membrane mimetic were evaluated. In DPC micelles, this ratio is higher than 1 (i.e., 1.13), which indicates that the peptide could present a coiled-coil structure-like profile or the helices are close to each other.[34,35] In addition, in POPC liposomes, the CD spectra of the peptide indicated a lower $[\theta]_{222}/[\theta]_{208}$ ratio (0.69), which excludes a coiled coil formation and indicates that this membrane mimetic stabilizes a more extended structure of the peptide.

The different CD spectra of the peptide in either micelles or liposomes indicate that distinct conformations are adopted by the peptide when incorporated into these environments. The difference in the structures could be caused either by environmental-induced changes or by peptide aggregation, with the latter possibility being excluded due to the confirmed peptide/micelles interaction, demonstrated in a previous study,[14] and the lower $[\theta]_{222}/[\theta]_{208}$ ratio found for the CD spectra of the peptide. The smaller curvature of the phospholipids in liposomes could promote a lower stabilization of the α helix structure of the peptides and indicated an increase of disorder in the peptide sequence when compared to micelles, as suggested by the CD data.

To confirm and further explore the conformational changes evidenced by the CD data, double electron–electron resonance (DEER)[28] spectroscopy was performed with samples containing the peptide/membrane mimetic systems. In this case, the dual labeled [Cys^{35}MTSL-$TOAC^0$]N-t(DH) peptide was used and the distances between the two spin labels in that peptide analogue were determined. The CD spectra for the peptide N-t(DH) and for the labeled analogue were similar in both membrane mimetic employed, suggesting that there is no significant structural perturbation due to the site specific attachment of TOAC and MTSL in the analogue. Figure 2 shows the four pulse DEER data for the peptide analogue [Cys^{35}MTSL-$TOAC^0$]N-t(DH) and shows the experimental spectra and theoretical fits of the time domain DEER traces. The insets of each graph present the distance distributions obtained from Tikhonov regularization.[30]

The time domain DEER data before background correction along with the background used for the correction and L-curve are included in Supporting Information (see Figures S1 and

S2). Inspection of the time domain data in Figure 2, parts A and B, suggest that there is a significant difference in the two data sets. The DEER modulation drops down much faster for the peptide in DPC micelles, when compared to POPC liposomes. Thus, indicating significant conformational changes are adopted by the peptide in these two different membrane environments. However, there is initial decay in the time domain of Figure 2B close to the modulation depth of ~1.5%—which is similar to the decay in Figure 2A—indicating that some minor population of peptide in liposomes may adopt the conformation similar to the micelles. Further analysis of the DEER data of the spin-labeled peptide analogue revealed a significant difference in the spin–spin distances in the two membrane mimetic environments. The average distances between the two spin labels are significantly shorter in micelle (32 Å), when compared to liposome (48 Å). The uncertainty of the distances is approximately ±4 Å. The full widths of distribution at half maxima (fwhm) are ~16 Å for micelle sample and ~13 Å for the major liposome sample peak. These wider distance distributions may be due to the multiple rotameric conformation of the MTSL spin label and the flexibility of the peptides.[27,36–38] The distance distribution plot in Figure 2B also revealed some minor populations close to the distance distribution obtained in Figure 2A. The minor distance peaks observed in the DEER distance distribution plot may be due to the contribution of a more disordered peptide structure and/or may be some contribution from the peptide having conformation similar to that of the micelle sample.

The major distance peak observed in the liposome sample is at approximately ~48 Å, which is close to the DEER detection limit of the liposome samples.[29] The distance distribution is greatly dependent on the background correction function used in the data analysis program. A two-dimensional background function was used for the liposome sample following the method previously published in the literature[17,27,28,39] and the instruction manual for the DEER data analysis program.[29] Since the two spin labels used in this study have different motional/dynamic environments (MTSL being more mobile whereas TOAC being more rigid), the use of single spin labeled DEER data as background would not be very helpful. In addition, we also examined the regularization parameter close to the turning points in the L-curve. The uncertainty in these distances was estimated by examining the regularization parameter in the L-curve, background functions and the reproducibility of the sample preparation.

CONCLUSIONS

The differences in the peptide structural organization as indicated by the CD data in micelles and liposomes (Figure 1) along with the differences in the distance distribution observed for the peptide analogue via DEER (Figure 2) suggest that the peptide mimicking the *Hs*DHODH N-terminal microdomain adopts conformations that are membrane environment specific. As the N-terminal microdomain presents two helices, $\alpha 1$ and $\alpha 2$, the difference in the distances between the two spin labels, located in helices, could indicate different conformations of the helices between micelles and liposomes. This could suggest that this microdomain would recognize specific and more ordered regions of the mitochondria membrane, thus probably adopting a more open conformation that, in turn, could be related to facilitate the quinone access to the *Hs*DHODH active site.

In conclusion, we successfully demonstrated the existence of conformational changes in the *Hs*DHODH N-terminal microdomain using peptide analogues in micelles and liposomes. These differences in the secondary structures were further explored with DEER spectroscopic technique and clearly confirmed by the distinct distances in the different model membranes examined. Micelles are considered simplistic membrane mimetic environments that are reasonable for demonstrating small secondary structures in peptides. Alternatively, liposomes represent a more complete and real model of membranes for large domain interactions.[40] To the best of our knowledge, this is the first study to report on conformational changes on the *Hs*DHODH N-terminal microdomain as evidenced by the combination of CD and DEER spectroscopic techniques.

Supplementary Material

Refer to Web version on PubMed Central for supplementary material.

Acknowledgments

This work was generously supported and funded by CAPES (Coordenação de Aperfeiçoamento de Pessoal de Nível Superior) with PDSE/BEX scholarship Process Number 6834/12-4 (to E.F.V.), CNPq (Conselho Nacional de Desenvolvimento Científico e Tecnológico), FAPESP (Fundação de Amparo à Pesquisa do Estado de Saõ Paulo) Process Number 10/06526-6 (to E.M.C.), National Institutes of Health Grants R01 GM108026 (to G.A.L.), and National Science Foundation (NSF) Grant CHE-1305664 (to G.A.L.). The pulsed EPR spectrometer was purchased through the NSF and the Ohio Board of Regents grants MRI-0722403 (to G.A.L.).

References

1. Loffler M, Fairbanks LD, Zameitat E, Marinaki AM, Simmonds HA. Pyrimidine pathways in health and disease. Trends Mol Med. 2005; 11(9):430–437. [PubMed: 16098809]
2. Malmquist NA, Gujjar R, Rathod PK, Phillips MA. Analysis of flavin oxidation and electron-transfer inhibition in *Plasmodium falciparum* dihydroorotate dehydrogenase. Biochemistry. 2008; 47(8):2466–2475. [PubMed: 18225919]
3. Hansen M, Le Nours J, Johansson E, Antal T, Ullrich A, Loffler M, Larsen S. Inhibitor binding in a class 2 dihydroorotate dehydrogenase causes variations in the membrane-associated N-terminal domain. Protein Sci. 2004; 13(4):1031–1042. [PubMed: 15044733]
4. Fairbanks LD, Bofill M, Ruckemann K, Simmonds HA. Importance of ribonucleotide availability to proliferating T-lymphocytes from healthy humans. Disproportionate expansion of pyrimidine pools and contrasting effects of de novo synthesis inhibitors. J Biol Chem. 1995; 270(50):29682–29689. [PubMed: 8530356]
5. Goldenberg MM. Leflunomide, a novel immunomodulator for the treatment of active rheumatoid arthritis. Clin Ther. 1999; 21(11):1837–1852. [PubMed: 10890256]
6. Shawver LK, Schwartz DP, Mann E, Chen H, Tsai JM, Chu L, Taylorson L, Longhi M, Meredith S, Germain L, Jacobs JS, Tang C, Ullrich A, Berens ME, Hersh E, McMahon G, Hirth KP. Inhibition of platelet-derived growth factor-mediated signal transduction and tumor growth by N-[4-(trifluoromethyl)-phenyl] 5-methylisoxazole-4-carboxamide. Clin Cancer Res. 1997; 3(7):1167–1177. [PubMed: 9815796]
7. Couto SG, Nonato MC, Costa Filho AJ. Defects in vesicle core induced by *Escherichia coli* dihydroorotate dehydrogenase. Biophys J. 2008; 94(5):1746–1753. [PubMed: 17993483]
8. McLean JE, Neidhardt EA, Grossman TH, Hedstrom L. Multiple inhibitor analysis of the brequinar and leflunomide binding sites on human dihydroorotate dehydrogenase. Biochemistry. 2001; 40(7): 2194–2200. [PubMed: 11329288]
9. Cowen D, Bedingfield P, McConkey GA, Fishwick CWG, Johnson AP. A study of the effects of substituents on the selectivity of the binding of N-arylaminomethylene malonate inhibitors to DHODH. Bioorg Med Chem Lett. 2010; 20(3):1284–1287. [PubMed: 20034791]

10. Liu SP, Neidhardt EA, Grossman TH, Ocain T, Clardy J. Structures of human dihydroorotate dehydrogenase in complex with antiproliferative agents. Struct Fold Des. 2000; 8(1):25–33.
11. Rawls J, Knecht W, Diekert K, Lill R, Loffler M. Requirements for the mitochondrial import and localization of dihydroorotate dehydrogenase. Eur J Biochem. 2000; 267(7):2079–2087. [PubMed: 10727948]
12. Diao YY, Lu WQ, Jin HT, Zhu JS, Han L, Xu MH, Gao R, Shen X, Zhao ZJ, Liu XF, Xu YF, Huang J, Li HL. Discovery of Diverse Human Dihydroorotate Dehydrogenase Inhibitors as Immunosuppressive Agents by Structure-Based Virtual Screening. J Med Chem. 2012; 55(19): 8341–8349. [PubMed: 22984987]
13. Couto SG, Nonato MC, Costa Filho AJ. Site directed spin labeling studies of *Escherichia coli* dihydroorotate dehydrogenase N-terminal extension. Biochem Biophys Res Commun. 2011; 414(3):487–492. [PubMed: 21986535]
14. Vicente EF, Nobre TM, Pavinatto FJ, Oliveira ON, Costa-Filho AJ, Cilli EM. N-Terminal Microdomain Peptide from Human Dihydroorotate Dehydrogenase: Structure and Model Membrane Interactions. Protein Pept Lett. 201410.2174/09298665216661405081252l5
15. Merrifield RB. Solid phase peptide synthesis. I. The synthesis of a tetrapeptide. J Am Chem Soc. 1963; 85(14):2149–2154.
16. Carpino LA, Han GY. The 9-Fluorenylmethoxycarbonyl amino-protecting group. J Org Chem. 1972; 37(22):3404–3409.
17. Sahu ID, McCarrick RM, Troxel KR, Zhang R, Smith HJ, Dunagan MM, Swartz MS, Rajan PV, Kroncke BM, Sanders CR, Lorigan GA. DEER EPR measurements for membrane protein structures via bifunctional spin labels and lipodisq nanoparticles. Biochemistry. 2013; 52(38): 6627–32. [PubMed: 23984855]
18. Schreier S, Bozelli JC Jr, Marín N, Vieira RFF, Nakaie CR. The spin label amino acid TOAC and its uses in studiesof peptides: chemical, physicochemical, spectroscopic,and conformational aspects. Biophys Rev. 2012; 4(1):45–66. [PubMed: 22347893]
19. Vicente EF, Basso LG, Cespedes GF, Lorenzon EN, Castro MS, Mendes-Giannini MJ, Costa Filho AJ, Cilli EM. Dynamics and conformational studies of TOAC spin labeled analogues of Ctx(Ile^{21})-Ha peptide from Hypsiboas albopunctatus. PLoS One. 2013; 8(4):e60818. [PubMed: 23585852]
20. Vieira RFF, Casallanovo F, Cilli EM, Paiva ACM, Schreier S, Nakaie CR. Conformational studies of TOAC-labeled bradykinin analogues in model membranes. Lett Pept Sci. 2002; 9(2–3):83–89.
21. Vieira RFF, Casallanovo F, Marin N, Paiva ACM, Schreier S, Nakaie CR. Conformational Properties of Angiotensin II and Its Active and Inactive TOAC-Labeled Analogs in the Presence of Micelles. Electron Paramagnetic Resonance, Fluorescence, and Circular Dichroism Studies. Biopolymers. 2009; 92(6):525–537. [PubMed: 19728302]
22. Ghimire H, Hustedt EJ, Sahu ID, Inbaraj JJ, McCarrick R, Mayo DJ, Benedikt MR, Lee RT, Grosser SM, Lorigan GA. Distance measurements on a dual-labeled TOAC AChR M2 delta peptide in mechanically aligned DMPC bilayers via dipolar broadening CW-EPR spectroscopy. J Phys Chem B. 2012; 116(12):3866–3873. [PubMed: 22379959]
23. Georgieva ER, Ramlall TF, Borbat PP, Freed JH, Eliezer D. Membrane-bound alpha-synuclein forms an extended helix: long-distance pulsed ESR measurements using vesicles, bicelles, and rodlike micelles. J Am Chem Soc. 2008; 130(39):12856–7. [PubMed: 18774805]
24. Rusu L, Gambhir A, McLaughlin S, Radler J. Fluorescence correlation spectroscopy studies of peptide and protein binding to phospholipid vesicles. Biophys J. 2004; 87(2):1044–1053. [PubMed: 15298909]
25. Crusca E Jr, Rezende AA, Marchetto R, Mendes-Giannini MJS, Fontes W, Castro MS, Cilli EM. Influence of N-terminus modifications on the biological activity, membrane interaction and secondary structure of the antimicrobial peptide Hylin-a1. Biopolymers. 2011; 96(1):41–48. [PubMed: 20560142]
26. Nowinski AK, Sun F, White AD, Keefe AJ, Jiang SY. Sequence, Structure, and Function of Peptide Self-Assembled Monolayers. J Am Chem Soc. 2012; 134(13):6000–6005. [PubMed: 22401132]
27. Sahu ID, McCarrick RM, Lorigan GA. Use of Electron Paramagnetic Resonance To Solve Biochemical Problems. Biochemistry. 2013; 52(35):5967–5984. [PubMed: 23961941]

28. Jeschke G. DEER Distance measurements on proteins. Annu Rev Phys Chem. 2012; 63:419–446. [PubMed: 22404592]
29. Jeschke G, Chechik V, Ionita P, Godt A, Zimmermann H, Banham J, Timmel CR, Hilger D, Jung H. DeerAnalysis2006 - a comprehensive software package for analyzing pulsed ELDOR data. Appl Magn Reson. 2006; 30:3–4. 473–498.
30. Chiang YW, Borbat PP, Freed JH. The determination of pair distance distributions by pulsed ESR using Tikhonov regularization. J Magn Reson. 2005; 172(2):279–295. [PubMed: 15649755]
31. Ingallinella P, Bianchi E, Finotto M, Cantoni G, Eckert DM, Supekar VM, Bruckmann C, Carfi A, Pessi A. Structural characterization of the fusion-active complex of severe acute respiratory syndrome (SARS) coronavirus. Proc Natl Acad Sci U S A. 2004; 101(23):8709–14. [PubMed: 15161975]
32. Chin DH, Woody RW, Rohl CA, Baldwin RL. Circular dichroism spectra of short, fixed-nucleus alanine helices. Proc Natl Acad Sci USA. 2002; 99(24):15416–21. [PubMed: 12427967]
33. Deluca D, Woehlke G, Moroder L. Synthesis and conformational characterization of peptides related to the neck domain of a fungal kinesin. J Pept Sci. 2003; 9(4):203–11. [PubMed: 12725241]
34. Greenfield NJ, Hitchcock-DeGregori SE. Conformational intermediates in the folding of a coiled-coil model peptide of the N-terminus of tropomyosin and alpha alpha-tropomyosin. Protein Sci. 1993; 2(8):1263–73. [PubMed: 8401212]
35. Suzuki K, Hiroaki H, Kohda D, Tanaka T. An isoleucine zipper peptide forms a native-like triple stranded coiled coil in solution. Protein Eng. 1998; 11(11):1051–5. [PubMed: 9876926]
36. Fleissner MR, Bridges MD, Brooks EK, Cascio D, Kalai T, Hideg K, Hubbell WL. Structure and dynamics of a conformationally constrained nitroxide side chain and applications in EPR spectroscopy. Proc Natl Acad Sci USA. 2011; 108(39):16241–16246. [PubMed: 21911399]
37. Mchaourab HS, Steed PR, Kazmier K. Toward the Fourth Dimension of Membrane Protein Structure: Insight into Dynamics from Spin-Labeling EPR Spectroscopy. Structure. 2011; 19(11): 1549–1561. [PubMed: 22078555]
38. Sahu ID, Kroncke BM, Zhang RF, Dunagan MM, Smith HJ, Craig A, McCarrick RM, Sanders CR, Lorigan GA. Structural Investigation of the Transmembrane Domain of KCNE1 in Proteoliposomes. Biochemistry. 2014; 53(40):6392–6401. [PubMed: 25234231]
39. Sahu ID, Hustedt EJ, Ghimire H, Inbaraj JJ, McCarrick RM, Lorigan GA. CW dipolar broadening EPR spectroscopy and mechanically aligned bilayers used to measure distance and relative orientation between two TOAC spin labels on an antimicrobial peptide. J Magn Reson. 2014; 249:72–79. [PubMed: 25462949]
40. Mijajlovic M, Wright D, Zivkovic V, Bi JX, Biggs MJ. Microfluidic hydrodynamic focusing based synthesis of POPC liposomes for model biological systems. Colloids Surf B. 2013; 104:276–281.

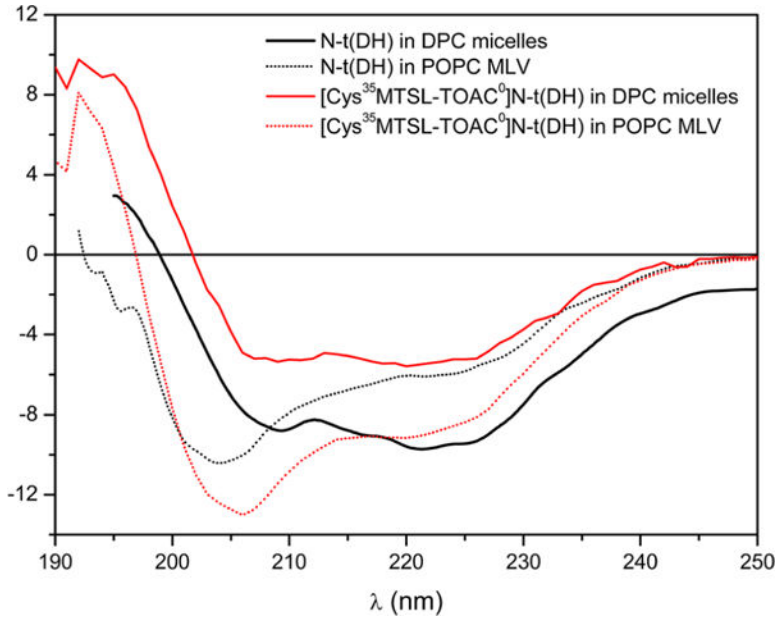

Figure 1.

CD spectra comparison of the peptide N-t(DH) (in black) and the doubly labeled analogue [Cys^{35}MTSL-$TOAC^{0}$]N-t(DH) (in red) in DPC micelles (concentration at 10 mmol L^{-1}) (solid lines) and POPC MLV liposomes (dotted lines) at 1:250 peptide/lipid ratio.

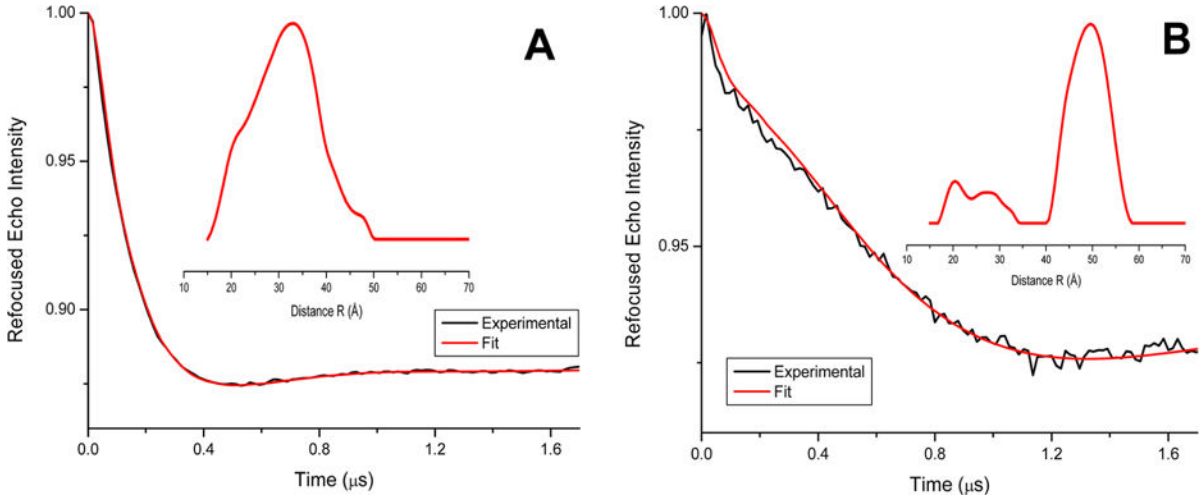

Figure 2.

Four pulse Q-band DEER data for the peptide analogue [Cys^{35}MTSL-TOAC^{0}]N-t(DH), representing the background-subtracted dipolar evolutions of the spins. Inset, the distance probability distributions from Tikhonov regularization are indicated for (A) DPC micelles (concentration at 10 mmol L^{-1}) and (B) POPC liposomes at 1:250 peptide/lipid ratio.